

VOLTAGE CONTROLLED-BANDWIDTH ELECTROOPTIC TRANSVERSE PHASE MODULATOR WITH PARALLEL ELECTRODES

التحكم بالجهد في النطاق الترددي لمعدل الزاوية الكهروضوئي المستعرض مع الأقطاب المتوازية

A. M. Zaghloul

Lecturer of Electronics and Communications, Faculty of Engineering, Zagazig University

د. عادل زغلول محمود - كلية الهندسة - جامعة الزقازيق

الخلاصة : في هذا البحث تم استخدام الجوارثم لإيجاد النطاق الترددي لمعدل الزاوية الكهروضوئي المستعرض. النطاق الترددي بحسب بإيجاد ثابت الانتشار لدليل الموجه المستطيل مع المواد الكهروضوئية وذلك قبل وبعد تسليط الجهد الكهربائي خلال الأقطاب المعدنية المتوازية. تم عمل التصميم الأمثل وذلك بإيجاد نطاق ترددي عريض واقل جهد مطلوب لإحداث تغيير في زاوية الطور بمقدار π (V_{π}) واقل مفاوئد. وجد أن KNbO_3 أفضل المواد الكهروضوئية التي تعطي أكبر نطاق ترددي وأقل رقم استحقاق ($V_{\pi}/\Delta F$) في حالة عدم دوران المحاور مع Z-cut. أما في حالة دوران المحاور BaTiO_5 تكون الأفضل مع Y-cut. وجد أيضا أن أداء المعدل يقل مع زيادة الطول الموجي وذلك لزيادة V_{π} على الرغم من زيادة النطاق الترددي. معامل الانتشار تقريبا لا يعتمد على مادة الأقطاب المعدنية والفضة تعطي أقل مفاوئد. تأثير طول المعدل يمكن التغلب عليه بتغيير الجهد الكهربائي المسلط بمعكوس نفس نسبة التغيير في طول المعدل وذلك في حالة عدم دوران المحاور. كما وجد أن المجال الكهربائي في اتجاه x يعطي نفس النتائج كما في اتجاه y مع تغيير حالات توجيه المحاور.

ABSTRACT: An algorithm to find the bandwidth (ΔF) and half wave retardation ($V_{\pm\pi}$) of the transverse phase modulator for several electrooptic materials with X, Y and Z-cuts, is cast where ΔF and $V_{\pm\pi}$ are calculated by determining the propagation constant of anisotropic metal clad electrooptic rectangular waveguide before (β_0) and after (β) applied voltage through parallel electrodes. The optimum design with broad ΔF , lower $V_{\pm\pi}$ and smallest propagation losses is done. It is found that KNbO_3 without rotating of axes (Z-cut) is the best material but, BaTiO_5 with rotating of axes (Y-cut) gives smallest figure of merit ($V_{\pi}/\Delta F$). The values of ΔF , $V_{\pm\pi}$ and $V_{\pi}/\Delta F$ are increased with the operating wavelength (λ). The propagation constant approximately, is independent of the electrode material and silver gives smallest losses. Either E_x or E_y give similar numerical results with exchange the orientation cases. The effect of modulator length can be treated by change the applied voltage with the same reciprocal ratio without rotating of axes.

1- INTRODUCTION

High speed electrooptic (EO) modulator is essential for future optical communication on systems [1-5]. Modulation bandwidth (ΔF) is a critical factor when dense wavelengths channels are to be multiplexed onto the same optical beam, so fast switching speed and wide bandwidth are useful in advanced telecommunication systems [6]. The development of large broadband with lower $V_{\pm\pi}$ modulators and minimum propagation losses are the major considerations [7-9]. Transverse phase modulator is the simplest EO modulator, it consists of an EO material placed between parallel electrodes [10] as shown in

Fig.1. The electric field is applied along one of the crystal's principle axes, light polarized along any other principle axes, an index of refraction change, hence an optical path length change and so, a change in propagation delay is done and that is proportional to the applied electric field [8]. LiNbO_3 , LiTaO_3 , KNbO_3 (Z-cut), BaTiO_3 , BaTiO_5 (Y-cut) are the optimum EO materials for studied isotropic and anisotropic materials [11-13]. Metal electrodes behaves as a high loss dielectric with a negative dielectric constant over the entire frequency range of light [12], accordingly, metal cladding on the wave-guide provides significant propagation loss. Metal electrode

losses can be reduced by inserting a dielectric film (buffer layer) with lower refractive index (n_b) between the waveguide and the electrode as shown in Fig.2. Loss of TM mode is very high than losses of TE mode, so, buffer layer must be used with TM mode [12]. Although the best direction for TM mode is parallel with the electrode not perpendicular with it. Aluminum (Al), copper (Cu), gold (Au) and silver (Ag) metal electrodes are used and silver losses are very small. The propagation constant can be considered approximately, independent of the kind of material of metal electrodes. Propagation losses are approximately, independent of the EO material. In this algorithm the calculation of the change of propagation constant is the difference between the propagation constants after and before the applied electric field. The values of bandwidth (ΔF) and half wave retardation ($V_{\pm\pi}$) for the above five materials are studied with optical polarized E_{pq}^x (to avoid the very large losses of TM mode) and applied electric field in y-direction, E_y , (where, results with E_x are the same results of E_y

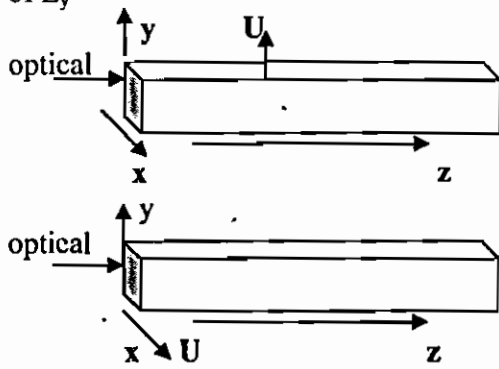


Fig.1 Transverse phase modulator with Parallel electrodes (propagation in z-direction) E_y (V in y-direction), E_x (V in x-direction)

with exchange the orientation cases). The values of $V_{\pm\pi}$ and ΔF depend upon the case of orientation axes. Case 1 gives the best figure of merit for LiNbO₃, LiTaO₃ and KNbO₃, while case 4 gives the best results for BaTiO₃ ($r_{41}=r_{51}=820$) and BaTiO₅ ($r_{41}=r_{51}=1700$). The results of the present algorithm is in good agreement if it is compared with that calculated by $\Delta\beta = k_0 \Delta n_z$ [15].

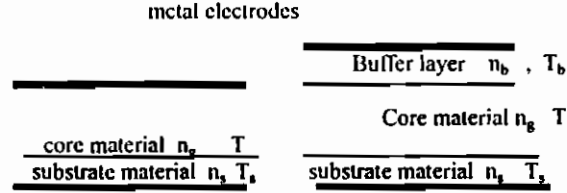


Fig.2 Slab waveguide with and without buffer layer

2- MATHEMATICAL ANALYSIS

2.1 Electrooptic Effect: When an electric field is applied upon EO material a new index ellipsoidal (IE) shape occurred, where there are changed in both scale and orientation from original one. The new IE with linear EO effect (Pockel's effect) is [16];

$$\begin{aligned} & (n_a^{-2} + r_{11}E_a + r_{12}E_b + r_{13}E_c)a^2 \\ & + (n_b^{-2} + r_{21}E_a + r_{22}E_b + r_{23}E_c)b^2 \\ & + (n_c^{-2} + r_{31}E_a + r_{32}E_b + r_{33}E_c)c^2 \\ & + 2(r_{41}E_a + r_{42}E_b + r_{43}E_c)bc \\ & + 2(r_{51}E_a + r_{52}E_b + r_{53}E_c)ac \\ & + 2(r_{61}E_a + r_{62}E_b + r_{63}E_c)ab = 1 \end{aligned} \quad (1)$$

Where; E_a , E_b and E_c are the electric field components in a, b and c directions. where, a, b and c are the crystallographic axes, so, there are six positions (cases) for the orientation of coordinate system axes (x, y and z) with respect to crystallographic axes. Z-cut (Case1: x//a, y//c, z//b, and case3: x//c, y//a, z//b), Y-cut (case2: x//b, y//c, z//a, case4: x//c, y//b, z//a) and X-cut (case5: x//a, y//b, z//c, case 6: x//b, y//a, z//c).

2.1.1 IE for EO materials which have point group symmetry (3m)

Such as LiNbO₃ and LiTaO₃ becomes;

$$\begin{aligned} & (n_a^{-2} + r_{12}E_b + r_{13}E_c)a^2 + (n_b^{-2} + r_{22}E_b + r_{23}E_c)b^2 \\ & + (n_c^{-2} + r_{33}E_c)c^2 + 2(r_{42}E_b)bc + 2(r_{51}E_a)ac \\ & + 2(r_{61}E_a)ab = 1 \end{aligned} \quad (2)$$

2.1.2 IE for EO materials which have point group symmetry (mm2, 4mm, 6mm)

Such as KNbO₃, BaTiO₃, BaTiO₅, ZnO and m-NA becomes;

$$\begin{aligned} & (n_a^{-2} + r_{13}E_c)a^2 + (n_b^{-2} + r_{23}E_c)b^2 + (n_c^{-2} + r_{33}E_c)c^2 \\ & + 2(r_{42}E_b)bc + 2(r_{51}E_a)ac = 1 \end{aligned} \quad (3)$$

2.1.3 IE for EO material which have point group symmetry (23, 4'2m, 4'3m)

Such as ADP, KDP, KDP^a, GaAs and Bi₁₂SiO₂₀ becomes;

$$\begin{aligned} & (n_a^{-2})a^2 + (n_b^{-2})b^2 + (n_c^{-2})c^2 + 2(r_{41}E_a)bc \\ & + 2(r_{52}E_b)ac + 2(r_{63}E_c)ab = 1 \end{aligned} \quad (4)$$

The axes rotating by angle θ , to eliminate the cross products of xy , xz and yz and this angle depends on the applied voltage (except for case 6 for LiNbO_3 and LiTaO_3 where, $\theta = 45$ degree regardless the value of E_y). So, cases 3, 4 and 6 can not be controlled by applied voltage. But these cases (absolute value of $\theta > 0$) are studied to find the comparison between electrooptic materials.

2.2 Changes of Refractive Index With Parallel Electrodes

For electric field in y -direction E_y , and from Eqs.3 and 4, there is not index change for EO material which have point groups 23, 4'2m and 4'3m (ADP, KDP, KDP^a and GaAs) and cases 5 and 6 for materials with point groups 6mm, 4mm and mm2 (BaTiO_3 , BaTiO_5 , KNbO_3 , m-NA and ZnO). The change of refractive index Δn_x and Δn_y for several point groups are indicated in Table.1 which indicates that, for LiNbO_3 and LiTaO_3 , cases 1 and 2 are similar ($n_a=n_b$, $r_{13}=r_{23}$), cases 5 and 6 are similar ($n_a=n_b$, $r_{61}=r_{12}=-r_{22}$) and case 1(case 2) is the best case where, cases 3 and 4 need largest value of E_y to overcome the smallest value of 0 and case 5 (case 6) with very small r_{12} and r_{22} . Also Table 1 indicates that, for BaTiO_3 and BaTiO_5 , cases 1 and 2 are similar ($n_a=n_b$, $r_{13}=r_{23}$), cases 3 and 4 are similar ($n_a=n_b$, $r_{42}=r_{51}$) and case 1 (case2) gives good change of refractive index where, $r_{33}=105$ (BaTiO_5). Cases 3 and 4, have very excellent values of $r_{42}=r_{52}=1700$ (BaTiO_5), with smallest θ (θ increased with E_y) which decrease the effect of largest values of r_{42} . So, the best case is case 4. For KNbO_3 , case 1 is the optimum case, where case 1 with $r_{33}=64$, $r_{13}=28$, case 2 with $r_{23}=1.3$, so, the index change can occurred in one direction. But the largest value of $r_{42}=380$ can not be useful with E_y , especially the difference $n_x^2 - n_y^2$ has large value (0.0286) with case 4. Finally, optimum cases with E_y are, case 1 (LiNbO_3 , LiTaO_3 and KNbO_3), but case 4 (BaTiO_3 and BaTiO_5). To prove that, the numerical results of Δn_x and Δn_y with electric field equal $1\text{V}/\mu\text{m}$ are indicated in Table 2.

2.3 Propagation Constant and Losses for Metal Clad Waveguide

Relative permittivity of metal electrode is complex ($\epsilon_m = \epsilon_{mr} + j\epsilon_{mi}$) and it is a function of wavelength (λ) [11] as;

$$\epsilon_{mr} = 1 - \omega_p^2 / (\omega^2 - \omega_i^2),$$

$$\epsilon_{mi} = -\omega_p^2 \omega_i / (\omega^3 + \omega \omega_i^2) \tag{5}$$

Where ω_p is the plasma frequency and ω_i is the collision damping frequency. $\omega_p = 19.8 \cdot 10^{15}$, $10.1 \cdot 10^{15}$, $9.9 \cdot 10^{15}$ and $12.2 \cdot 10^{15}$, but $\omega_i = 1.01 \cdot 10^{15}$, $0.31 \cdot 10^{15}$, $0.44 \cdot 10^{15}$ and $0.09 \cdot 10^{15}$ for aluminum, copper, gold and silver, respectively [11]. The minimum values of wavelength (λ_{min}) which give negative values for ϵ_{mr} are 0.0953 , 0.1867 , 0.1906 and $0.1545 \mu\text{m}$ for aluminum, copper, gold and silver, respectively, so, ϵ_{mr} for the above four metals usually negative within the range of optical wavelength for optical communication (i.e. $\lambda = 0.5 \mu\text{m}$ to $2.0 \mu\text{m}$) as shown in Appendix A, and ϵ_{mi} usually negative. Refractive index of metal is complex

$$n_m = n_{mr} - jn_{mi}, \quad n_m^2 = \epsilon_m = \epsilon_{mr} + j\epsilon_{mi}$$

where, $\epsilon_m < 0, \epsilon_{mi} < 0$ (6)

2.3.1 Calculations of propagation constant, β , and losses, α , for isotropic slab waveguide without buffer layer (Fig.2)

The characteristic equation of slab waveguide without buffer can be derived as;

$$k_y T = (q+1)\pi - \tan^{-1} k_y A_s / \gamma_s - \tan^{-1} k_y A_m / \gamma_m$$

where, $k_y = k_0(n_g^2 - N_y^2)^{0.5}$, $k_0 = 2\pi/\lambda$, $\gamma_s = k_0(N_y^2 - n_s^2)^{0.5}$, $\gamma_m = k_0(N_y^2 - \epsilon_{mr})^{0.5} E_1/\eta_r$, $E_1 = [1 + \epsilon_{mi}^2 / (N_y^2 - \epsilon_{mr})^2]^{0.5}$, $\eta_{r,1} = (\pm 0.5 + 0.5E_1)^{0.5}$ (7)

$A_s = A_m = 1$ (TE mode), $A_s = (n_s/n_g)^2$, $A_m = (\epsilon_{mr} - \epsilon_{mi} \eta_i / \eta_r) / n_g^2$ (TM mode), q is the mode number and N_y is the effective index of the waveguide, so, propagation constant is given by;

$$\beta = k_0 N_y \tag{8}$$

By using Newton- Raphson method mixed with try and error method, Eq.7 can be solved to give β . The attenuation factor (α) and losses are defined as [12]:

$$\alpha = - [(q+1)\pi / T^2] [k_y A_m \eta_i / (\eta_r \beta \gamma_m)] \tag{9.a}$$

$$\text{Losses} = 8.685 |\alpha| \text{ dB/cm} \tag{9.b}$$

2.3.2 Calculations of propagation constant, β , and losses, α , with buffer layer

Characteristic equation for isotropic slab waveguide with buffer (Fig.2) is the same equation of slab without buffer but by replacing $\gamma_m g_b$ instead of γ_m in Eq.7 [12] where;

$$g_b = [1 + (\gamma_m / \gamma_b A_b) \tanh(\gamma_b T_b)] / [1 + (\gamma_b A_b / \gamma_m) \tanh(\gamma_b T_b)]. \quad (10)$$

where, $\gamma_b = k_0(N_y^2 - n_b^2)^{0.5}$, $A_b = 1$ (TE mode), and $A_b = (\epsilon_{mr} - \epsilon_{mi} \eta_i / \eta_r) / n_b^2$ (TM mode) (11) special case, for very well wave guide (more confinement of light through wave guide) N_y approach n_g so, $A_s k_y / \gamma_s \ll$,

$$A_m k_y / \gamma_m \ll \text{ and so, Eq.7 converted into, } k_y T = (q+1)\pi - k_y A_s / \gamma_s - k_y A_m / \gamma_m. \quad (13)$$

so, $k_y^2 = (q+1)^2 \pi^2 [1 + A_s / (T \gamma_s) + A_m / (T \gamma_m)] / T^2$. β is defined in [12] as $\beta^2 = k_0 n_g^2 - k_x^2$ (14) then,

$$\beta = k_0 n_g - (q+1)^2 \pi^2 [1 - 2A_s / (T \gamma_s) - 2A_m / (T \gamma_m)] / (2k_0 n_g T^2). \quad (15)$$

The dependence of losses on the waveguide parameters are plotted in Appendix A, which indicates that losses independent approximately, of n_b , n_s and n_g specially at lower wavelength. Losses of TM mode are very greater than that of TE mode. Losses increased with λ but it decreased with T and T_b as suggested. Losses of silver are the smallest value.

2.4 Propagation Constant of Anisotropic Metal Clad Rectangular Waveguide
To avoid the greater loss of TM mode, the analysis is done for E_{pq}^x mode (i.e. TM mode in x-direction and TE mode in y-direction) with anisotropic materials (Fig.3). The propagation constant is defined as [13]; $\beta = (\beta_x^2 + \beta_y^2 + A)^{0.5}$ (16) where, β_x ($\beta_x = k_0 N_x$) and β_y ($\beta_y = k_0 N_y$) are the propagation constants and effective refractive indices for slabs in x and y directions, respectively, with modified refractive index distribution (Fig.3). Characteristic equations for slabs in x (TM mode) and y (TE mode) directions are,

$$k_x W = (p+1)\pi - 2 \tan^{-1}(n_s^2 k_x / n_{gx}^2 \gamma_x) \quad (17)$$

$$k_y T = (q+1)\pi - \tan^{-1}(k_y / \gamma_s) - \tan^{-1}(k_y / \gamma_m g_b) \quad (18)$$

where $g_b = 1$ if $T_b = 0$

N_x is the solution of Eq. 17, and N_y is the solution of Eq. 18. where,

$$\begin{aligned} k_x &= k_0 (n_{gz} / n_{gx}) (0.5 n_{gx}^2 - N_x^2)^{0.5} \\ \gamma_x &= k_0 (n_{gz} / n_{gx}) (N_x^2 + 0.5 n_{gx}^2 - n_s^2)^{0.5} \\ k_y &= k_0 (0.5 n_{gx}^2 - N_x^2)^{0.5} \\ \gamma_s &= k_0 (N_x^2 + 0.5 n_{gx}^2 - n_s^2)^{0.5} \\ \gamma_m &= k_0 (N_x^2 + 0.5 n_{gx}^2 - \epsilon_{mr})^{0.5} E_1 / \eta_r \\ E_1 &= [1 + \epsilon_{mi}^2 / (N_y^2 + 0.5 n_{gx}^2 - \epsilon_{mr})^2]^{0.5} \\ \eta_r &= (0.5 + 0.5 E_1)^{0.5} \\ \gamma_b &= k_0 (N_y^2 + 0.5 n_{gx}^2 - n_b^2)^{0.5} \end{aligned} \quad (19)$$

p and q are the mode numbers in x and y directions, respectively

$$A = V_1 / (V_2 V_3) \quad (20)$$

$$V_1 = 2 k_o^2 (n_{gx} / n_s)^4 \cos^2(k_x W / 2) * (n_{gx}^2 - n_s^2) (G_x + H_x).$$

$$V_2 = w + \sin(k_x w) / k_x + 2(n_{gx} / n_s)^4 \cos^2(k_x w / 2) / \gamma_x.$$

$$V_3 = T (1 + F_x^2) + (1 - F_x^2) \sin(k_y T) / k_y + G_x + H_x.$$

$$F_x = [\gamma_x / k_y \cos(k_y T / 2) - \sin(k_y T / 2)] / [\gamma_x / k_y \sin(k_y T / 2) + \cos(k_y T / 2)].$$

$$G_x = [\cos(k_y T / 2) + F_x \sin(k_y T / 2)]^2 / \gamma_s \text{ and } H_x = [\cos(k_y T / 2) - F_x \sin(k_y T / 2)]^2 / (g_b \gamma_m).$$

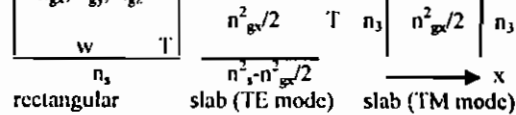


Fig.3 Anisotropic rectangular waveguide (buffer material, T_b , n_b), $n_s^2 = n_s^2 - n_{gx}^2 / 2$

2.5-Change of Propagation Constant and Phase Shift Due to EO Effect

When applied an electric field to EO waveguide, the change in refractive index (Δn) and the change of propagation constant $\Delta \beta$ are done. In this algorithm;

$$\Delta \beta = \beta_v (V=U) - \beta_0 (V=0) \quad (21)$$

V is the applied voltage.

Electric field strength E_y , through the EO material (thickness T, relative permittivity $\epsilon_r = \sqrt{\epsilon_x \epsilon_y}$ [17]) calculated in case of buffer layer (thickness T_b , and relative permittivity ϵ_b) as,

$$E_y = U / (T + T_b \epsilon_r / \epsilon_b) \quad (22)$$

Steps of calculation of $\Delta \beta$ and $\Delta \phi$ are;

- 1- Calculation of propagation constant (β_0) before applied voltage, $V=0$, (i.e. refractive indices are n_x and n_y),
- 2- Calculation of change of refractive indices in x and y directions Δn_x and Δn_y due to applied voltage.

- 3- Calculation of new refractive index distribution in x and y directions, by summation the change of refractive index to the original refractive index n_x (new) = $n_x + \Delta n_x$ and n_y (new) = $n_y + \Delta n_y$.
- 4- Calculation of propagation constant (β_v) with new refractive index, n_x (new) and n_y (new)
- 5- $\Delta\beta$ due to the perturbation $\Delta\epsilon$ (x,y) of the dielectric constant of the wave guide $\Delta\beta = \beta_v - \beta_0$.
- 6- The change of phase shift $\Delta\phi$ is;

$$\Delta\phi = \Delta\beta L_m \quad (23)$$
 Where, L_m is the modulator length

2.6 Evaluation of Modulation Depth (ζ) and Modulation Bandwidth (ΔF):

The modulation bandwidth of phase modulator is the difference between the upper and lower frequencies at which the modulation depth falls to 50% of its maximum value [14] and modulation depth (ζ) is defined as, $\zeta = \text{sinc}(\Delta F \cdot C / N L_m)$ (24)
 So, bandwidth $\Delta F = 0.6 v / (N L_m)$ (25)
 Where, v is the speed of light and N is the effective index of the modulator waveguide ($N = \beta / k_0$).

3- RESULTS AND DISCUSSION

For the calculation, we need the whole set of EO material parameters, such as elements of ϵ_j , r_{ij} , and n_i , we could not find a complete set of these parameters, especially the effect of λ on the last parameters, therefore, we use the following parameters, which we believe, are not too far from the real ones; [10]. Data of EO materials at $\lambda = 0.633 \mu\text{m}$ [11-12, 14-21] are: LiNbO_3 ($n_a = n_b = 2.286$, $n_c = 2.200$, $\epsilon_a = \epsilon_b = 43$, $\epsilon_c = 28$, $r_{12} = -6.8$, $r_{13} = 9.6$, $r_{22} = 6.8$, $r_{23} = 8.6$, $r_{33} = 30.9$, $r_{42} = 32.6, r_{51} = 32.6$, $r_{61} = 6.8$), LiTaO_3 ($n_a = n_b = 2.176$, $n_c = 2.180$, $\epsilon_a = \epsilon_b = 42$, $\epsilon_c = 41$, $r_{12} = -0.2$, $r_{13} = 8.4$, $r_{22} = 0.2$, $r_{23} = 8.4$, $r_{33} = 30.5$, $r_{42} = 20, r_{51} = 20$, $r_{61} = 0.2$), BaTiO_3 ($n_a = n_b = 2.41$, $n_c = 2.36$, $\epsilon_a = \epsilon_b = 2300$, $\epsilon_c = 60$, $r_{13} = 19$, $r_{23} = 19$, $r_{33} = 28$, $r_{42} = 820$, $r_{52} = 820$), BaTiO_5 ($n_a = n_b = 2.480$, $n_c = 2.426$, $\epsilon_a = \epsilon_b = 4300$, $\epsilon_c = 168$, $r_{13} = 14.5$, $r_{23} = 14.5, r_{33} = 105$, $r_{42} = 1700$, $r_{52} = 1700$), KNbO_3 ($n_a = 2.280$, $n_b = 2.329$, $n_c = 2.169$, $\epsilon_a = 160$, $\epsilon_b = 1000$, $\epsilon_c = 55$, $r_{13} = 28$, $r_{23} = 1.3$, $r_{33} = 64$, $r_{42} = 380$, $r_{51} = 105$) and LiNbO_3 at $\lambda = 1.15 \mu\text{m}$ ($n_a = n_b = 2.229$,

$n_c = 2.150$, $\epsilon_a = \epsilon_b = 43$, $\epsilon_c = 28$, $r_{12} = -5.4$, $r_{13} = 9.6$, $r_{22} = 5.4$, $r_{23} = 9.6$, $r_{33} = 30.9$, $r_{42} = 32.6$, $r_{51} = 32.6$, $r_{61} = 5.4$).

Note, in this paper we assume quasi-static operations. The results are evaluated with main example, waveguide width ($W = 8 \mu\text{m}$), waveguide thickness ($T = 8 \mu\text{m}$), buffer thickness ($T_b = 0 \mu\text{m}$, to avoid the mode conversion by T_b), wavelength ($\lambda = 0.633 \mu\text{m}$), mode numbers ($p = q = 0$), substrate material ($n_s = 1.502$), buffer material ($n_b = 1.446$) and aluminum metal electrode.

The propagation constant is independent approximately, of the material of electrode, also, silver gives the smallest losses (Table 3). Losses approximately independent of the EO materials. The effect of the applied voltage, V , on the change of propagation constant $\Delta\beta$ is indicated in Table 4, for the favorite cases of the five EO materials with aluminum electrodes and teflon buffer material. $\Delta\beta$ increased linearly with applied voltage for cases without axes rotation, but $\Delta\beta$ rapidly increased for cases which has rotating of axes. BaTiO_5 gives the largest change of propagation constant (case 4). For modulation applications it is more relevant to consider the voltage required for an optical retardation by π (half wave retardation, V_π) [10]. The values of applied voltage which give change of phase shift $\Delta\phi$ equal $\pm\pi$ are evaluated for the five EO materials and different orientation cases with modulator length $L_m = 1000 \mu\text{m}$ (Table 5). Bandwidth (ΔF) depends of the orientation of crystallographic axes, (Table 5). The appropriate modulation figure of merit is the ratio $V_\pi / \Delta F$, this ratio is generally more useful for comparing modulators than the power per unit bandwidth [6] (Table 5), which shows that for LiNbO_3 , LiTaO_3 and KNbO_3 , the maximum bandwidth occurred at case 4, but smallest V_π occurred at case 1, also, minimum figure of merit occurred at case 1 so, best case for LiNbO_3 and LiTaO_3 is case 1 (or case 2) and for KNbO_3 is case 1. But for BaTiO_3 and BaTiO_5 , maximum band-width, minimum V_π and minimum figure of merit occurred at case 4 (or case 3). Also, from Table 5, polarity of applied voltage effect on the performance of

modulator where, ΔF is decreased and figure of merit ($V_{\pi} / \Delta F$) increased with V_{π} but, vice versa with V_{π} because, for V_{π} the change of $\Delta\beta$ becomes negative and effective refractive index, N , decreased and from Eq.25, ΔF increased. Although, the best material is KNbO_3 (case 1 without rotating of axes) and BaTiO_5 , gives the smallest value of V_{π} and smallest value of figure of merit (case 4 with rotating of axes). But, we must note that LiNbO_3 is the famous material in the published papers and books, perhaps because, LiNbO_3 has industrial advantages and other natural properties than that for other materials.

The values of $V_{\pm\pi}$ increased with T_b and the percentage of this increasing (incr %) depend upon the value of $\epsilon_r = (\epsilon_x \epsilon_y)^{0.5}$ and so, incr % (BaTiO_5) > incr % (BaTiO_3) > incr % (KNbO_3) > incr % (LiTaO_3) > incr % (LiNbO_3) as indicated in Table 6. Effect of T_b on the performance of the modulator are shown in Table 7 which indicates that the values of $\Delta\phi$, ΔF , Δn_x , Δn_x and Δn_x decreased with T_b but vice versa for values of figure of merit ($V_{\pi} / \Delta F$) and β_v .

The required values of V_{π} increased rapidly with λ , but the change of ΔF increased slowly, with λ so, the values of $V/\Delta F$ increased rapidly with λ (Table 8) as suggested, because, at lower λ the magnitude of propagation constant β becomes large and so, any small change of applied voltage ΔV make large change of propagation constant $\Delta\beta$ and this means that for each λ there are $V_{\pm\pi}$ (Table 9). The data of refractive index and electrooptic coefficients at $\lambda=0.633 \mu\text{m}$ can be used at any λ , because n^3r approximately independent of λ through the useful range of λ as indicated in [19]. But there are some difference between the numerical results, for the available data of LiNbO_3 at $\lambda=0.633 \mu\text{m}$ and $\lambda=1.15 \mu\text{m}$ (Table 8). The values of refractive index

and electrooptic coefficients at $\lambda=0.633 \mu\text{m}$ are used with different values of λ , which we believe, are not too far from the real ones. As suggested performance of modulator ($V_{\pi} / \Delta F$) improvement with mode numbers p and q (Table 10) because, propagation constant decreased with p and q . The values of $V_{\pm\pi}$ depends upon the waveguide thickness T (because the applied electric field E_y depends on T) but, $V_{\pm\pi}$ approximately, independent on the waveguide width W (Table 11). The change of modulator length can be treated by varies the applied voltage with the reciprocal ratio for orientation cases without rotating of axes, because the change of propagation constant increased linearly with the applied voltage (Table 4). As example, for LiNbO_3 at $\lambda=0.633 \mu\text{m}$ with case 1, the phase shift ($\Delta\phi=1.5707 \text{ rad}$) occurred with either $L_m=1000 \mu\text{m}$ and $V=22.065 \text{ volt}$ or $L_m=500 \mu\text{m}$ and $V=44.13 \text{ volt}$

As a result of the applied voltage (i.e. E_y), there is a change of refractive index in z -direction (propagation direction) Δn_z so, this change makes change of propagation constant $\Delta\beta_z$ [15] as:

$$\Delta\beta = k_0 \Delta n_z \quad (\text{method 2}) \quad (26)$$

Where, Δn_z can be calculated directly from index ellipsoidal with some orientation cases. Method 2 is unable to give the propagation constant, effect of modulator width, effect of operating mode numbers and kind of mode, also, it used only for cases which has direct change in n_z (cases without rotating of axes) also for uniaxial materials. The results of $\Delta\beta$ by our algorithm are very good if it is compared with that by $\Delta\beta = k_0 \Delta n_z$, but results of KNbO_3 (biaxial material) are far from results by algorithm (Table 12) The numerical results with electric field E_x are similar with that by E_y , but, with exchange cases (Table 13).

Table 1: Change of refractive index with constant E_y ($E_x=E_z=0$) and propagation in z-direction, $A_n=(1/n_x^2-1/n_y^2)$. For any hidden cases the values of θ , Δn_x and Δn_y are zeros

Case	θ	$\Delta n_x / (0.5n_x^3)$	$\Delta n_y / (0.5n_y^3)$
LiNbO ₃ , LiTaO ₃ (3m)			
1	0	$-r_{13}E_y$	$-r_{33}E_y$
2	0	$-r_{23}E_y$	$-r_{33}E_y$
3	$0.5 \tan^{-1}(2r_{31}E_y/A_n)$	$[A_n \sin^2(\theta) - r_{31}E_y \sin 2\theta]$	$-[A_n \sin^2(\theta) - r_{31}E_y \sin 2\theta]$
4	$0.5 \tan^{-1}[2r_{42}E_y/(A_n - r_{22}E_y)]$	$[A_n \sin^2(\theta) - r_{42}E_y \sin 2\theta - r_{22}E_y \sin^2(\theta)]$	$-[A_n \sin^2(\theta) - r_{42}E_y \sin 2\theta - r_{22}E_y \sin^2(\theta)]$
5	0	$-r_{12}E_y$	$-r_{22}E_y$
6	$0.5 \tan^{-1}(2r_{61}E_y/A_n)$	$[A_n \sin^2(\theta) - r_{61}E_y \sin 2\theta]$	$-[A_n \sin^2(\theta) - r_{61}E_y \sin 2\theta]$
KNbO ₃ , BaTiO ₃ , BaTiO ₅ , ZnO, m-NA (mm2, 4mm, 6mm)			
1	0	$-r_{13}E_y$	$-r_{33}E_y$
2	0	$-r_{23}E_y$	$-r_{33}E_y$
3	$0.5 \tan^{-1}(2r_{31}E_y/A_n)$	$[A_n \sin^2(\theta) - r_{31}E_y \sin 2\theta]$	$-[A_n \sin^2(\theta) - r_{31}E_y \sin 2\theta]$
4	$0.5 \tan^{-1}(2r_{42}E_y/A_n)$	$[A_n \sin^2(\theta) - r_{42}E_y \sin 2\theta]$	$-[A_n \sin^2(\theta) - r_{42}E_y \sin 2\theta]$

Table 2 Values of θ , Δn_x and Δn_y with $E_y = 1 \text{ V}/\mu\text{m}$.

Case		Z-cut		Y-cut		X-cut	
		1	3	2	4	5	6
LiNbO ₃	1000 Δn_x	-0.05734	-0.00037	-0.05734	-0.00037	0.04062*	0.04062*
	1000 Δn_y	-0.16451	0.00042	-0.16451	-0.04020	-0.04062*	-0.04062
	θ degree	0	0.1225	0	0.1225	0	45
LiTaO ₃	1000 Δn_x	-0.04327	0.00267	-0.04327	0.00267	-0.00103*	-0.00103*
	1000 Δn_y	-0.15799	-0.00266	-0.15799	-0.00163	0.00103*	-0.00103*
	θ degree	0	-1.47859	0	-1.47897	0	45
KNbO ₃	1000 Δn_x	-0.16593	-0.00279	-0.00821	-0.02612		
	1000 Δn_y	-0.32653	0.00324	-0.32563	0.03234		
	θ degree	0	0.29792	0	0.77183		
BaTiO ₃	1000 Δn_x	-0.13298	-0.59214	-0.13298	-0.59214		
	1000 Δn_y	-0.18402	0.63058	-0.18402	0.63058		
	θ degree	0	6.27035	0	6.27035		
BaTiO ₅	1000 Δn_x	-0.11058	-2.68145	-0.11058	-2.68145		
	1000 Δn_y	-0.74960	2.86452	-0.74960	2.86452		
	θ degree	0	12.45890	0	12.45890		

case 5 similar with case 6 by rotate axes $\theta=45^\circ$, BaTiO₃ is the excellent material with case 4 as suggested.

Table 3: Effect of material of metal electrodes on the propagation constants and losses for anisotropic rectangular waveguide with $\lambda=1\mu\text{m}$, $T_b=0.1\mu\text{m}$, $\beta(\mu\text{m})^{-1}$ and 10^6 losses (dB/cm)

Case		1		2		3		4		5		6	
		Beta	Loss	Beta	Loss	Beta	Loss	Beta	Loss	Beta	Loss	Beta	Loss
LiNbO ₃	Al	14.3528	10.4	14.3528	10.4	13.8125	10.2	13.8125	10.2	14.3524	10.4	14.3524	10.4
	Cu	14.3528	10.0	14.3528	10.0	13.8125	10.0	13.8125	10.0	14.3524	10.0	14.3524	10.0
	Au	14.3528	14.6	14.3528	14.6	13.8125	14.6	13.8125	14.6	14.3524	14.6	14.3524	14.6
	Ag	14.3528	2.2	14.3528	2.2	13.8125	2.1	13.8125	2.1	14.3524	2.2	14.3524	2.2
LiTaO ₃	Al	15.1325	10.6	15.1325	10.6	14.8183	10.5	14.8183	10.5	15.1323	10.6	15.1323	10.6
	Cu	15.1325	10.0	15.1325	10.0	14.8183	10.0	14.8183	10.0	15.1323	10.0	15.1323	10.0
	Au	15.1325	14.6	15.1325	14.6	14.8183	14.6	14.8183	14.6	15.1323	14.6	15.1323	14.6
	Ag	15.1325	2.2	15.1325	2.2	14.8183	2.2	14.8183	2.2	15.1323	2.2	15.1323	2.2
KNbO ₃	Al	14.3091	10.4	14.6230	10.5	13.6053	10.1	13.6051	10.1	14.3083	10.4	14.6224	10.5
	Cu	14.3091	10.0	14.6230	10.0	13.6053	10.0	13.6051	10.0	14.3083	10.0	14.6224	10.0
	Au	14.3091	14.6	14.6230	14.6	13.6053	14.6	13.6051	14.6	14.3083	14.6	14.6224	14.6
	Ag	14.3091	2.2	14.6230	2.2	13.6053	2.1	13.6051	2.1	14.3083	2.2	14.6224	2.2
BaTiO ₃	Al	15.1325	10.6	15.1325	10.6	14.8183	10.5	14.8183	10.5	15.1323	10.6	15.1323	10.6
	Cu	15.1325	10.0	15.1325	10.0	14.8183	10.0	14.8183	10.0	15.1323	10.0	15.1323	10.0
	Au	15.1325	14.6	15.1325	14.6	14.8183	14.6	14.8183	14.6	15.1323	14.6	15.1323	14.6
	Ag	15.1325	2.2	15.1325	2.2	14.8183	2.2	14.8183	2.2	15.1323	2.2	15.1323	2.2
BaTiO ₅	Al	15.5726	10.7	15.5726	10.7	15.2333	10.6	15.2333	10.6	15.5723	10.7	15.5723	10.7
	Cu	15.5726	9.9	15.5726	9.9	15.2333	10.0	15.2333	10.0	15.5724	9.9	15.5724	9.9
	Au	15.5726	14.5	15.5726	14.5	15.2333	14.5	15.2333	14.5	15.5724	14.5	15.5724	14.5
	Ag	15.5726	2.2	15.5726	2.2	15.2333	2.2	15.2333	2.2	15.5723	2.2	15.5723	2.2

Table 4: Dependence of modulator characteristics on the applied voltage , U(volt), with orientation case 1, $\lambda=0.633\mu\text{m}$ and $T_b=0$.

	LiNbO ₃		LiTaO ₃		KNbO ₃		BaTiO ₃		BaTiO ₅	
	U=10	U=50	U=10	U=50	U=10	U=50	U=10	U=50	U=10	U=50
1000 $\Delta\beta$	-0.7114	-3.5572	-0.5360	-2.6836	-2.0580	-10.294	-1.6499	-8.2512	-1.3733	-6.8607
$\Delta\phi$ (rad)	-0.7114	-3.5572	-0.5360	-2.6836	-2.0580	-10.294	-1.6499	-8.2512	-1.3733	-6.8607
ΔF (GHZ)	78.76584	78.77572	82.7495	82.75774	78.97746	79.00623	74.7138	74.73443	72.60293	72.61912
U/ ΔF	0.12696	0.63470	0.12080	0.60417	0.12662	0.63286	0.13384	0.66904	0.13774	0.68850
β_v (μm^{-1})	22.68352	22.68209	21.59151	21.58936	22.62274	22.61450	23.91374	23.90714	24.60901	24.60353
Δn_x	-0.07168	-0.35839	-0.05409	-0.27046	-0.20742	-1.03708	-0.16622	-0.83110	-0.13823	-0.69115
Δn_y	-0.20514	-1.02820	-0.19749	-0.98746	-0.40817	-2.04084	-0.23002	-1.15012	-0.93701	-4.68512
Δn_z	-0.07168	-0.35839	-0.05409	-0.27046	-0.01026	-0.05132	-0.16622	-0.83110	-0.13823	-0.69115

Table 5: The values of bandwidth (ΔF), figure of merit ($V/\Delta F$) at V_{π} with different orientation axes. E_{∞}^x , $\lambda=0.633\mu\text{m}$, aluminum and $T_b=0$. * negative voltage

	Case	U (volt)	$\Delta\phi$ (rad)	ΔF (GHZ)	V/ ΔF (V/GHZ)	Θ (degree)	Beta (0) (μm^{-1})	Beta (u) (μm^{-1})
LiNbO ₃	1 and 2	44.13	$-\pi$	78.77428	0.5602	0	22.68423	22.68109
	3	234.14	$-\pi$	81.85501	2.8604	3.5655	21.82745	21.82745
	4	232.71	$-\pi$	81.85501	2.8430	3.59	21.82745	21.82745
	5 and 6	62.386	$+\pi$	78.75337	0.7927	0	22.68711	22.68711
	1 and 2*	-44.156	$+\pi$	78.75246	-0.5607	0	22.68423	22.68737
	LiTaO ₃	1 and 2	58.47	$-\pi$	82.75948	0.7065	0	21.59204
3		90.34	$+\pi$	82.58358	1.0939	-15.1256	21.63174	21.63489
4		90.34	$+\pi$	82.58358	1.0939	-15.1651	21.63174	21.63489
5 and 6		2458	$-\pi$	82.75944	29.7005	0	21.59205	21.5891
1 and 2*		-58.5	$+\pi$	82.73540	-0.7071	0	21.59204	21.59518
KNbO ₃		1	15.25	$-\pi$	78.98125	0.1931	0	22.62479
	2	306.50	$-\pi$	77.31934	3.9641	0	23.11102	23.10788
	3	85.405	$-\pi$	83.02501	1.0287	3.1676	21.52300	21.51986
	4	27.875	$-\pi$	83.02550	0.3357	2.6821	21.52287	21.51973
	1*	-15.25	$+\pi$	78.95931	-0.1931	0	22.62479	22.62794
	BaTiO ₃	1 and 2	19.05	$-\pi$	74.71845	0.2550	0	23.91539
3 and 4		5.831	$-\pi$	76.30212	0.0764	4.6046	23.41909	23.41595
1 and 2*		-19.025	$+\pi$	74.69884	-0.2547	0	23.91539	23.91853
BaTiO ₅		1, 2	22.88	$-\pi$	72.60814	0.3151	0	24.61039
	3 and 4	2.688	$-\pi$	74.22492	0.0362	4.4364	24.07438	24.07125
	1 and 2*	-22.91	$+\pi$	72.58960	-0.3156	0	24.61039	24.61235

Table 6: Effect of T_b on the values of V_{π} with E_{∞}^x , $\lambda=0.633\mu\text{m}$, aluminum and case 1

T_b	LiNbO ₃ $\epsilon_r=34.7$		LiTaO ₃ $\epsilon_r=41.5$		KNbO ₃ $\epsilon_r=95.6$		BaTiO ₃ $\epsilon_r=371.5$		BaTiO ₅ $\epsilon_r=849.9$	
	V_{π}	incr. %	V_{π}	incr. %	V_{π}	incr. %	V_{π}	incr. %	V_{π}	Incr. %
0.00	44.13		58.47		15.25		19.05		22.88	
0.05	48.70	110.36	65.81	112.55	19.54	128.13	40.16	210.81	81.01	354.06
0.10	53.28	120.73	73.15	125.11	23.80	156.07	61.29	321.73	139.13	608.10

Table 7: the dependence of $\Delta\phi$, ΔF , figure of merit ($V_{\pi}/\Delta F$), β_o , β_v , Δn_x , Δn_y and Δn_z upon T_b for E_{∞}^x , LiNbO₃ with case 1 and $U=20\text{V}$

T_b	$\Delta\phi$ (rad)	ΔF (GHZ)	U/ ΔF (V/GHZ)	Beta (0) (μm^{-1})	Beta (u) (μm^{-1})	1000 Δn_x	1000 Δn_y	1000 Δn_z
0.00	-1.424789	78.76832	0.253909	22.68423	22.68280	-0.14335	-0.41128	-0.14335
0.05	-1.291275	78.76788	0.253911	22.68422	22.68293	-0.12988	-0.37263	-0.12988
0.10	-1.178741	78.76750	0.253912	22.68422	22.68304	-0.11873	-0.34062	-0.11873
0.15	-1.087189	78.76718	0.253913	22.68422	22.68313	-0.10933	-0.31368	-0.10933
0.20	-1.005173	78.76690	0.253914	22.68422	22.68321	-0.10132	-0.29068	-0.10132
0.25	-0.938416	78.76667	0.253915	22.68422	22.68328	-0.09440	-0.27083	-0.09440

Table 8: Dependence of V_{π} , ΔF , figure of merit ($V_{\pi}/\Delta F$) and β_v upon λ for E_{∞}^x , LiNbO₃ with case 1, data at $\lambda=0.633\mu\text{m}$ and $T_b=0$. * results with data of LiNbO₃ at $\lambda=1.15\mu\text{m}$

$\lambda\mu\text{m}$	V_{π} Volt	$\Delta\phi$	ΔF GHZ	$V_{\pi}/\Delta F$ Volt/ GHZ	β_o beta at $V=0$	β_v beta at $V=V_{\pi}$
0.633	44.130	$-\pi$	78.77428	0.560206	22.68423	22.68109
1.00	69.670	$-\pi$	78.81491	0.883970	14.35287	14.34973
1.15	80.120	$-\pi$	78.83584	1.016290	12.47785	12.47471
1.15*	86.482*	$-\pi^*$	80.8562*	1.0696*	12.1661*	12.1630*
1.55	107.922	$-\pi$	78.90371	1.367768	9.250611	9.247470

Table 9: Values of V_{π} as a function of λ for the five materials with case 1 and $T_b=0$

	V_{π} Volt (at $\Delta\phi = -\pi$)			V_{π} Volt (at $\Delta\phi = \pi$)		
	$\lambda = 0.633 \mu\text{m}$	$\lambda = 1.0 \mu\text{m}$	$\Lambda = 1.55 \mu\text{m}$	$\lambda = 0.633 \mu\text{m}$	$\lambda = 1.0 \mu\text{m}$	$\Lambda = 1.55 \mu\text{m}$
LiNbO ₃	44.13	69.67	107.922	-44.156	-69.7025	-107.95
LiTaO ₃	58.47	92.37	143.01	-58.5	-92.312	-143.00
KNbO ₃	15.25	24.09	37.37	-15.25	-24.113	-37.36
BaTiO ₃	19.05	30.07	46.57	-19.025	-30.05	-46.55
BaTiO ₅	22.88	36.144	55.98	-22.91	-36.16	-55.98

Table 10: Dependence of V_{π} , ΔF , figure of merit ($V_{\pi} / \Delta F$) and β_v upon p and q for E^x_{00} , LiNbO₃ with case 1, $\lambda = 0.633 \mu\text{m}$ and $T_b=0$

P	Q	V_{π} Volt	$\Delta\phi$	ΔF GHZ	$V_{\pi} / \Delta F$ Volt/ GHZ	β_0 beta at $V=0$	β_v beta at $V=V_{\pi}$
0	0	44.130	$-\pi$	78.77428	0.560206	22.68423	22.68109
0	1	44.130	$-\pi$	78.80902	0.559961	22.67423	22.6109
1	0	44.090	$-\pi$	78.80926	0.559443	22.67416	22.67102
1	1	44.090	$-\pi$	78.84403	0.559205	22.66416	22.66102

Table 11: Dependence of V_{π} , ΔF , figure of merit ($V_{\pi} / \Delta F$) and β_v upon W and T for E^x_{00} , LiNbO₃ with case 1, $\lambda = 0.633 \mu\text{m}$ and $T_b=0$

W	T	V_{π} Volt	$\Delta\phi$	ΔF GHZ	$V_{\pi} / \Delta F$ Volt/ GHZ	β_0 beta at $V=0$	β_v beta at $V=V_{\pi}$
2	8	44.055	$-\pi$	78.94283	0.558049	22.63580	22.63266
4	8	44.090	$-\pi$	78.80869	0.559456	22.67432	22.67118
8	2	11.015	$-\pi$	78.93777	0.139540	22.63725	22.63411
8	4	22.045	$-\pi$	78.80811	0.279730	22.67449	22.67449
8	8	44.130	$-\pi$	78.77428	0.560208	22.68423	22.68109

Table 12: Comparison between results by our algorithm and results by $\Delta\beta=k_0 \Delta n_x$ for case 1, $\lambda = 0.633 \mu\text{m}$ and $T_b=0$

		LiNbO ₃	LiTaO ₃	KNbO ₃	BaTiO ₃	BaTiO ₅
	U	44.130	58.47	15.25	19.05	22.88
Our algorithm	$1000\Delta\beta$	-3.141403	-3.141403	-3.141403	-3.141403	-3.141403
	ΔF	78.77428	82.75948	78.98125	74.71845	72.60814
	$V_{\pi} / \Delta F$	0.560208	0.706505	0.193084	0.254957	0.315116
Method 2	$1000\Delta\beta$	-3.139711	-3.139388	-0.155374	-3.143081	-3.139315
	ΔF	78.75105	82.73261	77.28691	74.69861	72.58990
	$V_{\pi} / \Delta F$	0.560373	0.706735	0.197317	0.255025	0.315195

Table 13: Change of refractive index with constant E_x ($E_y=E_z=0$) and propagation in Z-direction, $A_n = (1/n_x^2 - 1/n_y^2)$. For any hidden cases the values of θ , Δn_x and Δn_y are zeros

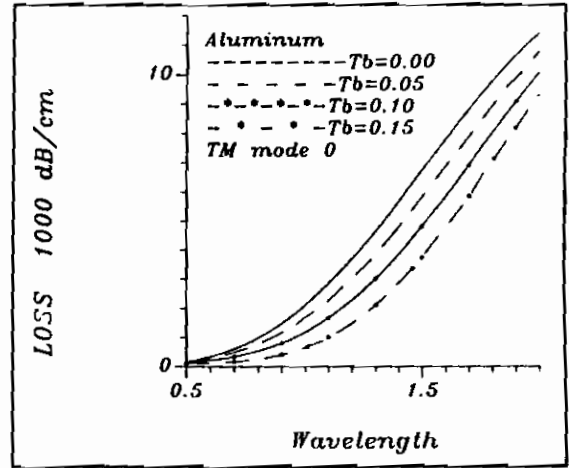
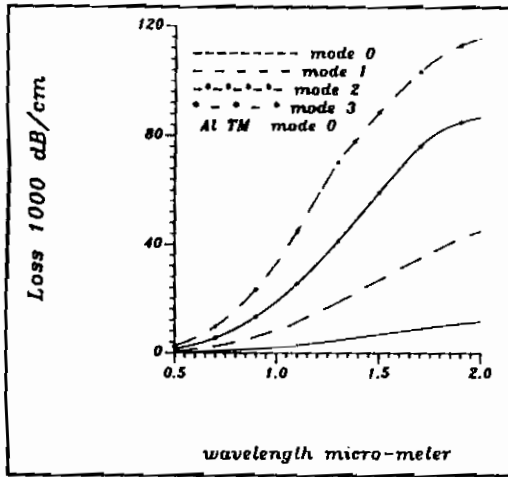
Case	θ	$\Delta n_x / (0.5n_x^3)$	$\Delta n_y / (0.5n_y^3)$
LiNbO3, LiTaO3 (3m)			
3	0	$-r_{33}E_x$	$-r_{13}E_x$
4	0	$-r_{33}E_x$	$-r_{23}E_x$
1	$0.5 \tan^{-1}(2r_{51}E_x/A_n)$	$[A_n \sin^2(\theta) - r_{51}E_x \sin 2\theta]$	$-[A_n \sin^2(\theta) - r_{51}E_x \sin 2\theta]$
2	$0.5 \tan^{-1}\{2r_{42}E_x / (A_n + r_{22}E_x)\}$	$[A_n \sin^2(\theta) - r_{42}E_x \sin 2\theta - r_{22}E_x \sin^2(\theta)]$	$-[A_n \sin^2(\theta) - r_{42}E_x \sin 2\theta + r_{22}E_x \sin^2(\theta)]$
6	0	$-r_{22}E_x$	$-r_{12}E_x$
5	$0.5 \tan^{-1}(2r_{61}E_x/A_n)$	$[A_n \sin^2(\theta) - r_{61}E_x \sin 2\theta]$	$-[A_n \sin^2(\theta) - r_{61}E_x \sin 2\theta]$
KNbO3, BaTiO3, BaTiO5, ZnO, m-NA (mm2, 4mm, 6mm)			
3	0	$-r_{33}E_x$	$-r_{13}E_x$
4	0	$-r_{33}E_x$	$-r_{23}E_x$
1	$0.5 \tan^{-1}(2r_{51}E_x/A_n)$	$[A_n \sin^2(\theta) - r_{51}E_x \sin 2\theta]$	$-[A_n \sin^2(\theta) - r_{51}E_x \sin 2\theta]$
2	$0.5 \tan^{-1}(2r_{42}E_x/A_n)$	$[A_n \sin^2(\theta) - r_{42}E_x \sin 2\theta]$	$-[A_n \sin^2(\theta) - r_{42}E_x \sin 2\theta]$

4-CONCLUSIONS

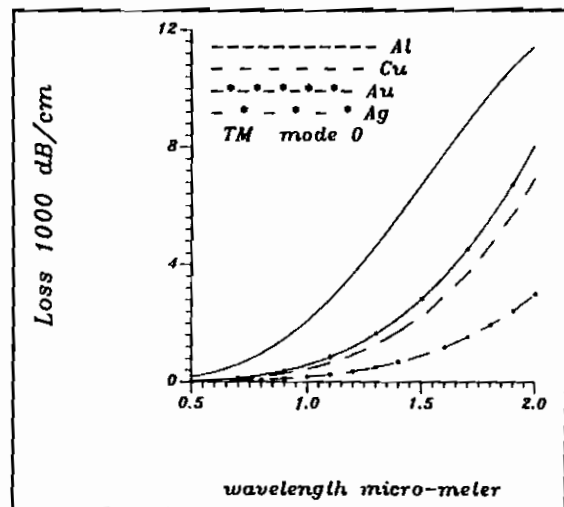
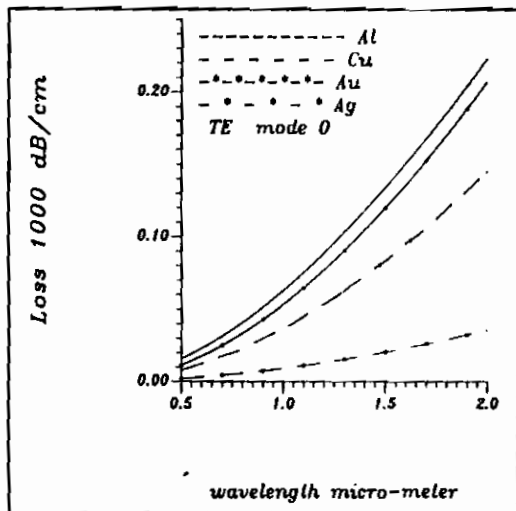
The designed algorithm is applied to compute the optimum transverse phase modulator (broad bandwidth, ΔF , lower V_{π} and smallest losses). Changes of propagation constant increase linearly with applied

voltage (without rotating of axes) so, the effect of modulator length can be treated by changing the applied voltage with the same reciprocal ratio. V_{π} and ΔF depend on the EO materials and orientation of axes. KNbO₃ with case 1 (without rotating of

Appendix A: continued



a- effect of mode number, $T_b=0$ b- effect of buffer thickness, $n_b=1.446$, $m=0$
 Fig.A.4 Effect of mode number (m) and buffer thickness (T_b) on the propagation losses for LiNbO₃ with Aluminum and TM mode. $T=8 \mu\text{m}$, $w=8 \mu\text{m}$, $n_s=1.502$, $n_g=1.532$.



a- TE mode b- TM mode
 Fig.A.5 Propagation losses of LiNbO₃ with Aluminum, Copper, Gold and Silver
 $T=8 \mu\text{m}$, $w=8 \mu\text{m}$, $T_b=0 \mu\text{m}$, $n_s=1.502$, $n_g=1.532$.